The analysis of possible nucleation processes indicates that oxygen recoil nuclei produced by the neutron component of cosmic rays act as nucleating agents.

The effects of lead or paraffin screens on the cavitation threshold are probably due to a decrease of the present neutron component reaching the liquid and to the production of secondaries in nuclear reactions induced by mesons and gamma rays in the screen material.

A cell formed by a liquid in an adequate sound field and suitably screened, constitutes a device which allows the examination of the influence of various penetrating particles entering the cell through a hole, on cavitation threshold. The device also allows one to distinguish the various types of particles: for example, its response to neutrons depends on their energy.

ACKNOWLEDGMENT

The authors express their thanks to Dr. M. Bertolotti for useful discussions.

PHYSICAL REVIEW VOLUME 125, NUMBER 2 JANUARY 15, 1962

# Harmonics of the Kruskal Limit and Field Diffusion in a Toroidal Pinch Discharge*

A. A. WARE,† H. K. FORSEN, AND A. A. SCHUPP
*John Jay Hopkins Laboratory for Pure and Applied Science, General Atomic Division of General Dynamics Corporation, San Diego, California*

(Received June 5, 1961)

Measurement of the magnetic fields in a toroidal pinch discharge have shown that when the applied toroidal magnetic field ($B_{z0}$) is comparable with or less than the self-field of the discharge ($B_\theta$), the $B_\theta$ field penetrates into the discharge more rapidly than expected by simple electromagnetic theory, and also the $B_z$ flux is enhanced within the discharge. This second effect was very marked in these experiments because of the high impedance of the supply circuit connected to the $B_z$ coils. In addition, the magnetic field oscillograms show steps which commence when the magnetic pitch ($\lambda_B=2\pi rB_z/B_\theta$) satisfied $\lambda_B\simeq L/n$ or $2L/n$, where $L$ is the torus circumference and $n$ is an integer. If it is assumed that instabilities prevent the formation of a large pressure gradient in the discharge, then $j_\perp \ll j_\parallel$, and the field configurations predicted for an applied electric field ($E_z$) are in good agreement with those observed experimentally after field penetration is complete. In particular, the enhancement of $B_z$ is explained. Further, the assumption of small $j_\parallel$ leads to the prediction of more rapid $B_\theta$ penetration at low $B_z$. The most likely instabilities which would cause the limitation in pressure gradient and produce the waveform steps are thought to be interchange modes.

## 1. INTRODUCTION

THEORY indicates that most pinch discharge configurations should be unstable to the $m=1$ mode of the magnetohydrodynamic kink instability. Even in discharges in which the currents are confined to a thin skin, the outer layers should be unstable to the $m=1$ mode unless the axial magnetic field ($B_z$) varies with radius according to stringent conditions and in particular changes sign within the current layer.[1] Experimentally, when discharges have been produced with little or no initial $B_z$, large amplitude kink instabilities have been observed by many workers following the initial discovery by Carruthers and Davenport[2] and Granovskii and Timofeeva.[3] In discharges with very high initial $B_z$, theory[4] predicts that the $m=1$ mode will be unstable for wavelengths in the $z$ direction ($2\pi/k$) greater than the pitch of the magnetic lines of force at the edge of the discharge, namely greater than $\lambda_B\equiv 2\pi aB_z/B_{\theta a}$, where $a$ is the radius of the discharge column and $B_{\theta a}$ the value of $B_\theta$ at this radius. When a toroidal discharge tube is used, a boundary condition is imposed limiting the possible wavelengths for the $m=1$ instability to the torus circumference ($L$) and submultiples of $L$. Hence, the onset of the $m=1$ mode will occur when $B_\theta$ has risen to the value which makes $\lambda_B=L$. (This is often referred to as the Kruskal limit.) Striking confirmation of the theory was obtained in experiments on the Stellarator by Kruskal *et al.*[5] More recently the higher $m$ modes have been detected[6] and these modes again appear at the critical values of $B_\theta$ predicted by theory; they cease at higher value of $B_\theta$, also in accordance with theory.

In the intermediate range where the initial $B_z$ is of

* Research on controlled thermonuclear reactions is a joint program carried out by General Atomic and the Texas Atomic Energy Research Foundation.

† Permanent Address: Limited Research Laboratory, Associated Electrical Industries, Berkshire, England.

[1] M. N. Rosenbluth, *Proceedings of the Second United Nations International Conference on the Peaceful Uses of Atomic Energy, Geneva, 1958* (United Nations, Geneva, 1958), Vol. 31, p. 85. See also B. R. Suydam, *ibid.*, Vol. 31, p. 157.

[2] R. Carruthers and P. A. Davenport, Proc. Phys. Soc. (London) **B70**, 49 (1957).

[3] V. L. Granovskii and G. G. Timofeeva, J. Exptl. Theoret. Phys. (USSR) **28**, 378 (1956).

[4] M. D. Kruskal and J. L. Tuck, Proc. Roy. Soc. **A245**, 222 (1958).

[5] M. D. Kruskal, J. L. Johnson, M. B. Gottlieb, and L. M. Goldman, reference 1, Vol. 32, p. 217.

[6] W. Bernstein, A. Z. Kranz, and F. Tenney, Phys. Fluids **3**, 1019 (1960).

the same order of magnitude as the value of $B_\theta$, a notable feature has been the absence of large amplitude magnetic field fluctuations (see Burkhardt and Lovberg,[7] Honsaker *et al.*,[8] Butt *et al.*,[9] and others). Small-amplitude fluctuations still remain, and it is an obvious inference that these are caused by the $m=1$ instability predicted for the outer layers by Rosenbluth,[1] but experimental proof for the identification is lacking. Partial evidence that an $m=1$ instability is occurring was obtained by Colgate *et al.*,[10] who observed that the characteristic abrupt increase in $B_z$ flux within the discharge still occurred. Such increases have been associated with $m=1$ instabilities in other experiments. Also, in the Zeta discharge, Butt has observed kinks on the gas current waveform at currents corresponding to the Kruskal limit and its harmonics.[11]

The generation of $B_z$ flux at the onset of an $m=1$ instability has not been explained theoretically. Similarly, the continuous enhancement of $B_z$ flux in the slow pinch discharge needs an explanation. If the discharge were highly constricted with a sharp edge, outside of which there was a good vacuum, the explanation would be simple. The unstable discharge would resemble a helical wire and the sense of the instability helix is such as to make the current confined to the wire enhance the original $B_z$. However, the experimental evidence is against both the highly constricted discharge and the vacuum regions. Another suggestion, that of continuous trapping of $B_z$, caused by the radial contraction of new plasma forming near the walls, also is an inadequate explanation, since it would not account for the negative $B_z$ fields often produced in the outer regions of the discharge. Some of the field enhancement can be explained by the paramagnetic effect of the nonisotropic conductivity of a plasma in a magnetic field,[12] but the observed currents in the $\theta$ directions are much larger than predicted by this effect, particularly in the outer regions of the discharge.[9,12]

A further feature of this type of discharge, particularly for toroidal tubes, is the rapid penetration of the $B_\theta$ field into the plasma, the rate exceeding that predicted by simple electromagnetic theory.[13] The discharge configuration degenerates rapidly to the approximately constant pitch magnetic field configuration associated with slow pinch discharges.[14] This constant pitch discharge is preserved in an approximately steady state for as long as the electric field is applied and an $m=1$ instability has been observed in the outer layers of such a discharge by Allen.[15]

In this paper some of the preliminary results obtained with a fast toroidal pinch discharge are presented. In particular, observations have been made on the enhancement of $B_z$ flux within the discharge and on the penetration of $B_\theta$. A notable feature on the magnetic probe oscillograms is the presence of kinks or steps at the Kruskal limit and its harmonics. To explain the field enhancement and penetration a simple theory is put forward which invokes instabilities merely as a mechanism to remove or prevent any appreciable pressure gradient in the discharge. The field configurations predicted for a discharge with small pressure gradient and $E_z$ constant with respect to radius are in good agreement with the experimental results. The possible causes of the pressure gradient limitation and the waveform steps are discussed.

## 2. DESCRIPTION OF APPARATUS

The experiments were carried out in an alumina torus with internal tube diameter of 7 cm and mean toroidal diameter of 51 cm. This was surrounded by a copper torus (internal tube diameter 8.4 cm) which was used as the primary to induce the gas current. This metal case had one gap running parallel to the $z$ direction and six gaps in the $\theta$ direction which divided the torus along the main circumference into six equal sectors. (Following the usual practice, to facilitate comparison with linear discharges, cylindrical co-ordinates are used to describe the discharge at a particular position along its length, the $z$ axis being taken at the center of the discharge tube and parallel to the main toroidal circumference at that point. Except where otherwise stated the toroidal curvature of the discharge tube is neglected.) To each of the six gaps was connected a condenser bank of 392 $\mu$F via standard ignitron switches. The condenser voltage used in these experiments was 5 kv. No iron core was used and the half period for the gas current was approximately 18 $\mu$sec.

A further condenser bank was connected to coils wound on the torus to produce a toroidal magnetic field. Inductances were connected in series with the condensers in this bank with a total effective inductance large compared with the inductance of the field coils. This was done so that further voltages could be applied to the field coils to program the magnetic field, but no such programming was done in the experiments described here. The half period of this field was 120 $\mu$sec. The switches in this circuit were closed first and the main gas current started about 50 $\mu$sec later. Considerable care was taken in the construction of the coils and the metal torus in order to keep stray fields from penetrating the discharge space. Measurements of the field showed the maximum deviations from a perfect toroidal field to be about 6% at the pump port. These perturbations were confined to regions near the gaps

[7] L. C. Burkhardt and R. H. Lovberg, Nature **181**, 228 (1958).
[8] J. Honsaker, H. Karr, J. Osher, J. A. Phillips, and J. L. Tuck, Nature **181**, 231 (1958).
[9] E. P. Butt, R. Carruthers, J. T. D. Mitchell, R. S. Pease, P. C. Thonemann, M. A. Bird, J. Blears, and E. R. Hartill, reference 1, Vol. 32, p. 42.
[10] S. A. Colgate, J. P. Ferguson, and J. P. Furth, reference 1, Vol. 32, p. 129.
[11] See G. Francis, *Proceedings of the Fourth International Conference on Ionization Phenomena in Gases, Uppsala, 1958* (North-Holland Publishing Company, Amsterdam, 1960), Vol. 2, p. 929.
[12] R. J. Bickerton, Proc. Phys. Soc. **72**, 618 (1958).
[13] D. J. Lees and M. G. Rusbridge, reference 11, Vol. 2, p. 876.
[14] A. A. Ware, Phys. Rev. **123**, 19 (1961).
[15] N. L. Allen, Nature **187**, 279 (1960).

and the pumping port and they were within a few millimeters of the tube wall. A fuller description of these fields and the torus construction will be given elsewhere.

The fields in the discharge were studied by a magnetic probe. The probe envelope was a 5-mm diam alumina tube, which was inserted in the equatorial plane of the torus and extended across the whole discharge tube. The probe contained 14 coils which were spaced to measure both $B_\theta$ and $B_z$ at the radii 0, $\pm 1$, $\pm 2$, $\pm 3$ cm. (The positive direction is radially outwards from the axis of rotation of the torus.) The coils were calibrated in a separate calibrating field and their signals were recorded on 7 double-beam oscilloscopes.

The gas used in these experiments was hydrogen. The initial pressures were in the range 0.015 to 0.15 mm Hg and the gas was pre-ionized by a 400-w rf oscillator.

## 3. EXPERIMENTAL RESULTS

### 3.1. Oscillograms

Figure 1 shows example oscillograms for the voltage applied to the torus and for the gas current. Over the ranges studied there was only a slow increase in current amplitude with increase in pressure and with increase in the initial axial magnetic field $B_{z0}$ (see Fig. 8). In Figs. 2–4 are example sets of the magnetic probe oscillograms for $B_\theta$ and $B_z$.

### 3.2. Spatial Distributions of Magnetic Field

In Figs. 5–7 are plots of $B_\theta$ and $B_z$ as functions of position at various times after the start of gas current. The small number of coil positions eliminates any fine structure, but the gross effects typical of this type of discharge are apparent. Among these are the enhancement of $B_z$ within the discharge and the rapid penetration of $B_\theta$.

At the high values of $B_{z0}$ only a very small increase in $B_z$ occurs in the discharge, but at low initial fields the increase is very marked. Thus, for $B_{z0}=0.17$ kgauss (Fig. 7) the field at the center of the discharge increases to more than 80 times its initial value, and the $B_z$ flux in the tube increases by about a factor of 37. The last

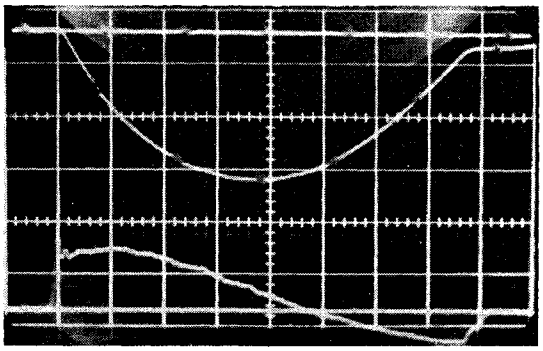

FIG. 1. Example oscillograms for the total gas current in the $z$ direction ($J_z$) and the voltage applied to the torus. The upper trace is $J_z$. The time base is 2 $\mu$sec per major division.

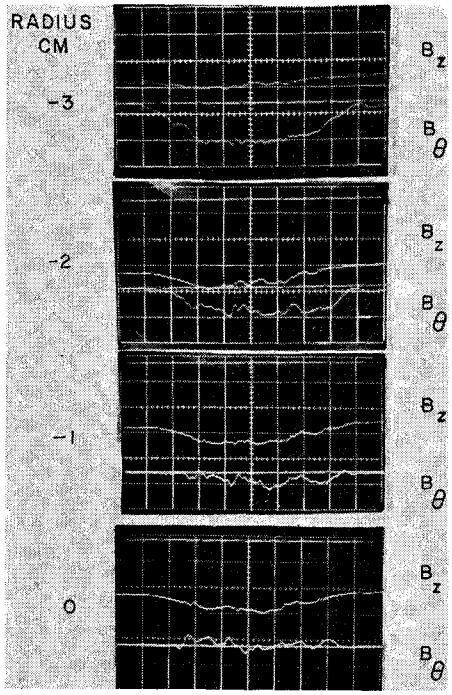


FIG. 2. Oscillograms for $B_z$ and $B_\theta$ at the radii indicated when the applied field ($B_{z0}$) was 11.6 kgauss.

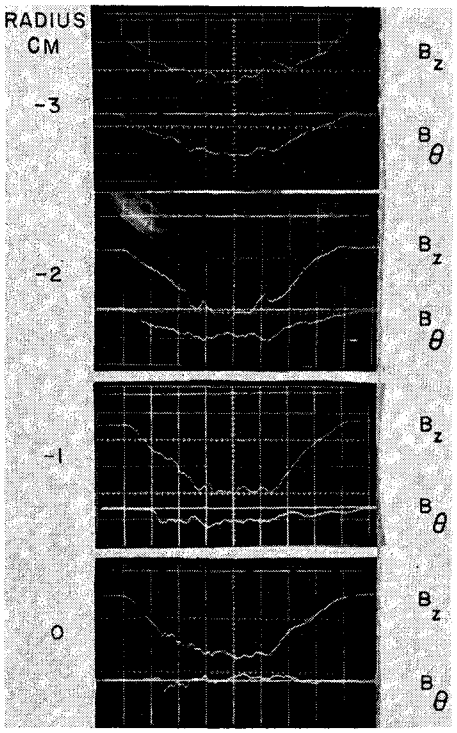


FIG. 3. Oscillograms for $B_z$ and $B_\theta$ when $B_{z0}$ was 2.6 kgauss.

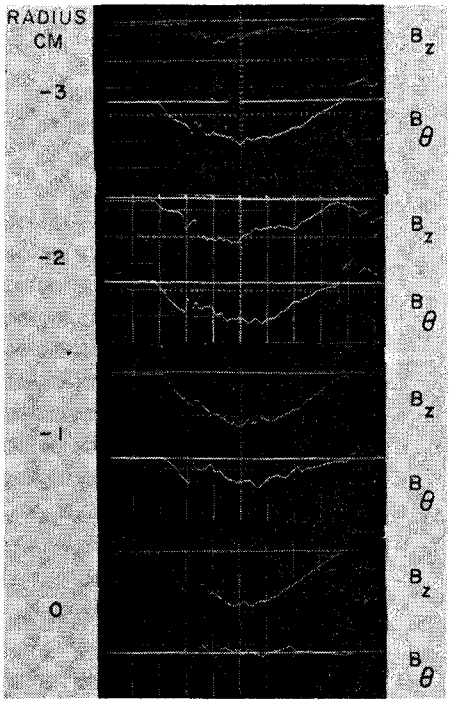


FIG. 4. Oscillograms for $B_z$ and $B_\theta$ when $B_{z0}$ was 0.3 kgauss.

result is a property peculiar to the experiment described here. In other pinch discharge experiments, it has been the general practice to use either a low impedance supply circuit for the coil producing the axial magnetic field or a metal screening cylinder continuous in the $\theta$

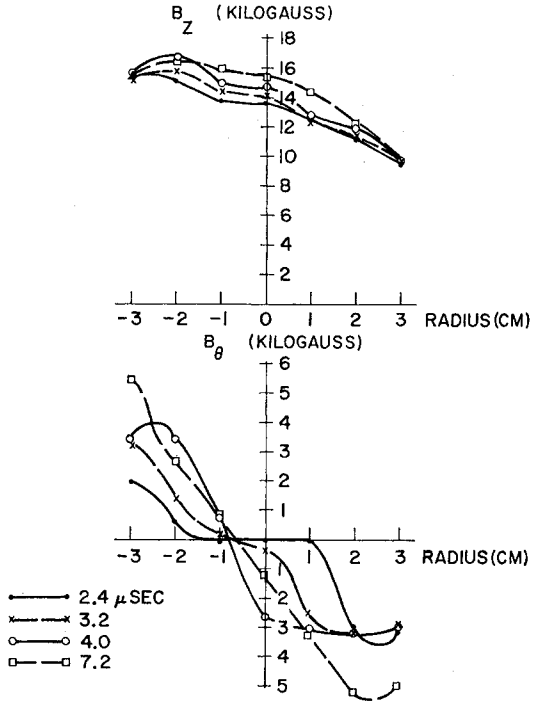


FIG. 5. Radial variation of $B_z$ and $B_\theta$ when $B_{z0}$ was 13 kgauss. The times are measured from the start of the current pulse.

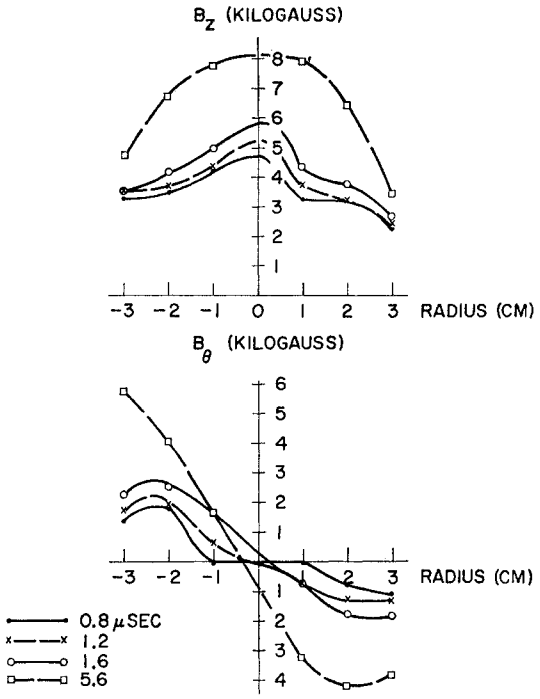


FIG. 6. Radial variation of $B_z$ and $B_\theta$ when $B_{z0}$ was 2.6 kgauss.

direction. The total $B_z$ in the tube is then kept approximately constant, and enhancement of $B_z$ in the center of the discharge is accompanied by a decrease in $B_z$ in the outer regions. In the present experiments the high impedance supply circuit maintained an approximately constant current despite the back emf due to the $\theta$ currents in the discharge. As a result the $B_z$ near the wall did not decrease appreciably and the large increase in total $B_z$ flux was possible.

In Fig. 8, $B_{zp}$, the peak value of $B_z$ at the center of the discharge at the time of peak current ($j_{zp}$) is plotted against the applied field ($B_{z0}$). Despite the two orders of magnitude change in the applied field the peak field varies by only a factor of 2. The variation of the total gas current in the $z$ direction is illustrated on the same graph.

The time for $B_\theta$ to penetrate the plasma and for the current density $j_z$ to take up an approximately uniform distribution, varied from about 1 $\mu$sec at the lowest values of $B_{z0}$ to about 4 $\mu$sec at 13 kgauss. A feature of the penetration is that while $B_\theta$ is increasing in the inner parts of the discharges, at the outer radii the value of $B_\theta$ remains approximately constant or increases only slowly. At the region of steep positive slope on the $B_\theta$ profile moves radially inwards it leaves a region with only small slope on the outside. In other words, the region of high $j_z$ travels inwards. When the penetration reaches the center, the current density there rises for a fraction of a microsecond to this high value and they drops back. This effect is particularly noticeable at high $B_{z0}$. Thus, in Fig. 9, which shows the $B_\theta$

profiles at 3.2, 4.0, and 4.8 $\mu$sec for the same conditions as Fig. 5, the slope at 4.0 $\mu$sec has risen to approximately twice the slope which occurs 0.8 $\mu$sec later when the approximately uniform current has been achieved. During this short interval (3.2–4.8 $\mu$sec) the applied voltage has dropped only 20%. The movement inwards of the region of high $j_z$ cannot be associated with the pinch effect since for this case $B_z > B_\theta$ and no appreciable constriction should occur.

### 3.3. Pitch of the Magnetic Lines of Force

The pitch ($\lambda_B$) of the helical lines of force in the case of a cylindrical discharge is $2\pi r B_z/B_\theta$. Here toroidal effects are neglected and the same formula is used to calculate the pitch. In order to determine the radius, $r$,

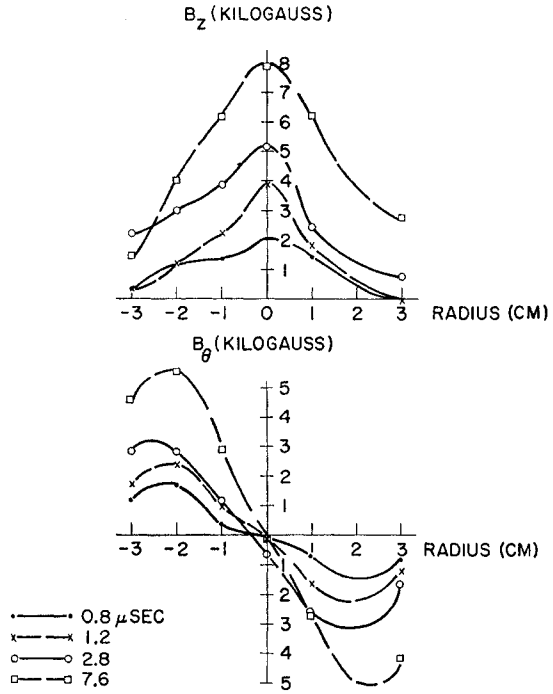


FIG. 7. Radial variation of $B_z$ and $B_\theta$ when $B_{z0}$ was 0.17 kgauss.

the center of the discharge was taken as the mean position throughout the current pulse for the zero of $B_\theta$. This mean position was generally close to the center of the tube, but in some cases at high $B_{z0}$ it was displaced towards the inner wall of the torus.

Figures 10–12 show $\lambda_B$ plotted as a function of time for various radii and $B_{z0}$. One of the major features of these graphs is the initial rapid decrease in $\lambda_B$ as $B_\theta$ penetrates into the discharge. In Fig. 10, a high $B_z$ case, it can be seen that the rapid decrease at the inner radius (1.5 cm) occurs when $\lambda_B$ for the outer radii is staying approximately constant. From about 4 $\mu$sec onwards $\lambda_B$ is approximately the same at all radii until within 3 $\mu$sec of the end of the half cycle, one exception being the irregularity at 9 $\mu$sec. At the end

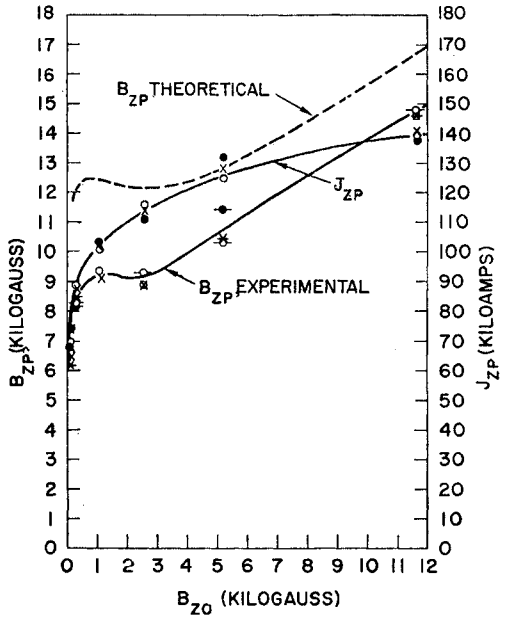


FIG. 8. The variation with $B_{z0}$ of the peak gas current ($J_{zp}$) and the peak value of $B_z$ at the center of the tube ($B_{zp}$). The broken curve shows the theoretical $B_{zp}$.

of the half cycle $\lambda_B$ stays small for a longer time near the center because the skin effect preserves the current longer in the center of the discharge. At intermediate values of $B_{z0}$ (Fig. 11) the behavior is similar, but after coming close together the values of $\lambda_B$ at different radii separate a small amount, there being a decrease of $\lambda_B$ with radius.

At low $B_{z0}$ there is an initial rapid drop in $\lambda_B$ to low

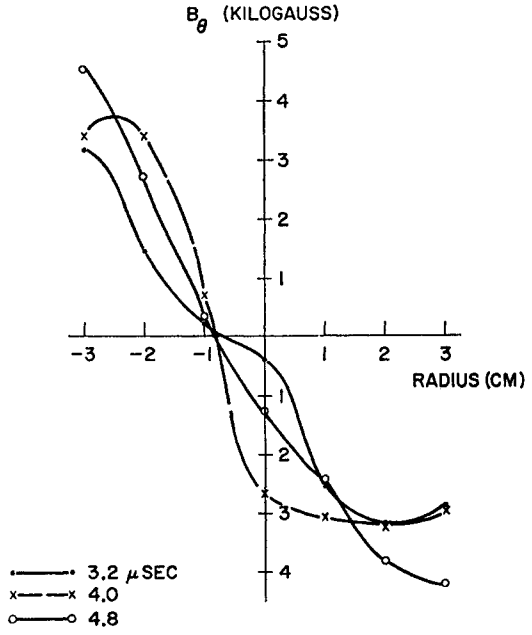


FIG. 9. Radial variation of $B_\theta$ for $B_{z0} = 13$ kgauss.

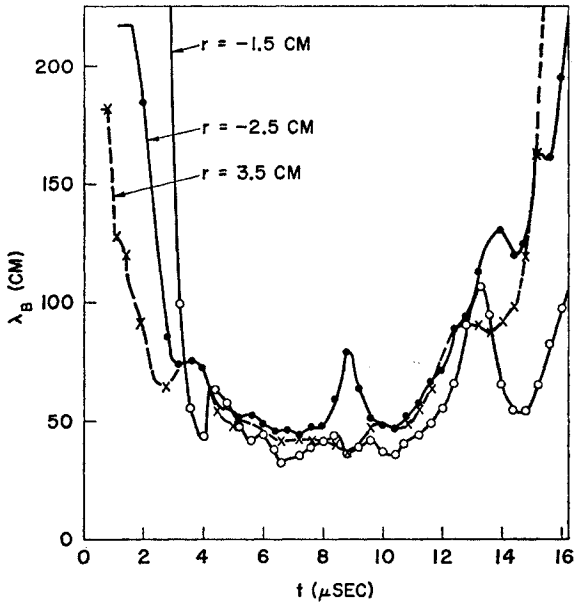


FIG. 10. Variation of the pitch of the magnetic field ($2\pi rB_z/B_\theta$) with time at the radii indicated. $B_{z0}$ was 13 kgauss.

values, but this is followed by an abrupt increase in $\lambda_B$. The latter is due to the abrupt increase in $B_z$ in the discharge (see the oscillograms for $B_z$ in Fig. 4). Following these initial changes, the fluctuations in the magnetic pitch are more erratic than with the larger $B_{z0}$. There is again a decrease of $\lambda_B$ with radius.

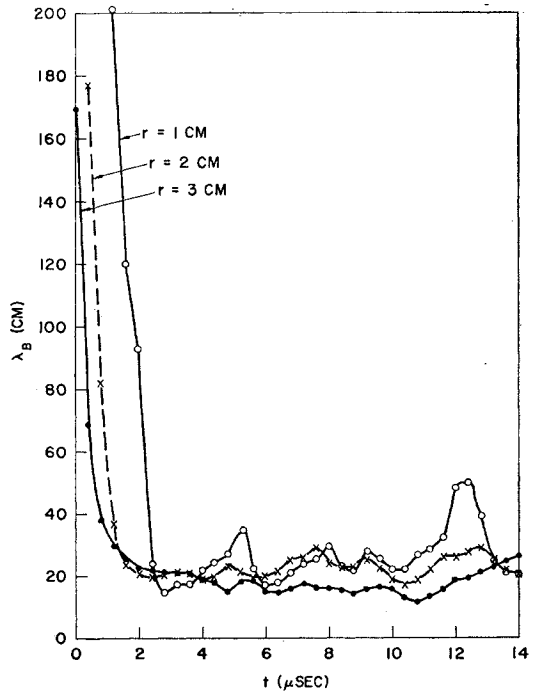


FIG. 11. Variation of the pitch of the magnetic field with time for $B_{z0}=2.6$ kgauss.

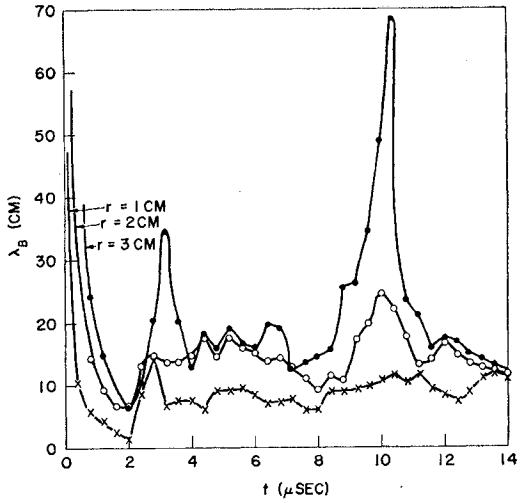


FIG. 12. Variation of the pitch of the magnetic field with time for $B_{z0}=0.17$ kgauss.

### 3.4. Steps in the Magnetic Field Oscillograms

A characteristic feature of the magnetic field oscillograms is the presence of kinks or steps on the waveforms. At high $B_{z0}$ the kinks are most obvious on the $B_\theta$ waveforms, but at low $B_{z0}$ they are apparent also on the $B_z$ signals. On the $B_\theta$ oscillograms for the larger radii $dB_\theta/dt$ often goes to zero at a kink so that the kinks look like steps, but sometimes $dB_\theta/dt$ remains positive and sometimes it goes negative. Occasionally the steps are very pronounced and have a regular appearance (see the examples in Fig. 13), but more often they are irregular.

The magnetic pitch has been calculated from the values of $B_\theta$ and $B_z$ at the beginning of each step on the $B_\theta$ waveforms. It has been found that in most cases there is a close correlation between these $\lambda_B$ and submultiples of the torus circumference. This can be seen from Table I where some example values of $\lambda_B$ for the steps have been arranged in columns according to the nearest submultiple of the torus circumference.

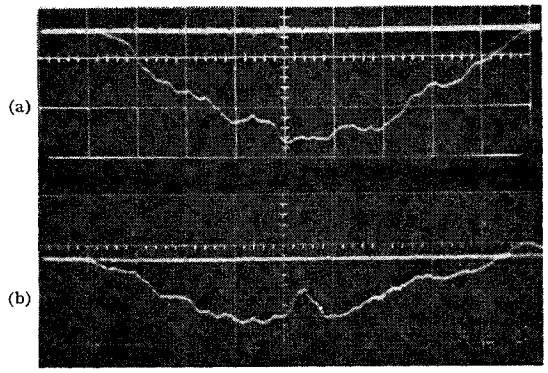


FIG. 13. Two examples of clearly defined steps on the $B_\theta$ waveform. Both are at the radius −3 cm. (a) $B_{z0}=8$ kgauss, (b) $B_{z0}=13$ kgauss.

TABLE I. Pitch of the magnetic field at steps in $B_\theta$ waveform ($\lambda_B$).[a]

| $B_z$ (kgauss) | Radius (cm) | Submultiples of torus circumference (cm) L/n, where n = 1, 2, 3 ··· | | | | | | | | | | | | | | | | | | |
|---|---|---|---|---|---|---|---|---|---|---|---|---|---|---|---|---|---|---|---|---|
| | | 160 | 80 | 53 | 40 | 32 | 26.6 | 22.9 | 20 | 17.8 | 16 | 14.5 | 13.3 | 12.3 | 11.4 | 10.7 | 10 | 9.4 | 8.9 | 8.4 | 8.0 |
| 11.6 | + 3 | 144 | 104 | 53 (47) (63) | 53 (45) | 42 | (36) | | | | | | | | | | | | | | |
| | - 3 | 144 | 94 (57) | 53 | 37.5 (34.5) | 33.5 | | | | | | | | | | | | | | | |
| 5.2 | + 3 | | 77 | 57 (46) | (34.5) | 30 | | 22.4 24.5 | 19.4 | 17.7 | | | | | | | | | | | |
| | - 3 | | 90 | 52 | 43 | (37) 30 | (28) 24.8 25.9 24.8 | 22.8 | 21.3 | | | | | | | | | | | | |
| 2.9 | + 3 | | | | | | 25.4 | | 21.2 | 18 | 16 | 14.1 14 | | | | | | | | | |
| | - 3 | | | | | 34 | 26.8 | 24.1 | 19.9 | 16.9 | 16.2 15.9 | | | | | | | | | | |
| 1.1 | + 3 | | | | | | | | | | | | | | 11.8 | | | 9.5 9.3 9.5 | | | 7.9 |
| | | | | | | | | | | | | | | | 10.6 | | 9.9 | 9.4 | | | |
| | - 3 | | | | | | | | | | | | 13.2 | | | | 9.9 10.1 9.9 | | | 8.4 | 7.9 |

[a] The arrows indicate the time sequence where this departs from the general decrease of $\lambda_B$ with time.

(The submultiples are $L/n$ where $L$ is the torus circumference (160 cm) and $n$ is an integer.) It can be seen that many of the values can be accounted for in this way. At the lowest values of $\lambda_B$ the spacing between adjacent values is of the same magnitude as the experimental error—the movements of the center of the discharge introduce a substantial error in the value taken for $r$—but it is significant that in the sequences, the spaces between the values of $\lambda_B$ vary in the correct manner. Most of the remaining values of $\lambda_B$ (those in brackets in Table I) fall roughly midway between the submultiples and can be fitted to the half-integral submultiples, namely $2L/n$. These occur mainly at high values of $B_{z0}$. Similar, but less distinct, steps occur in the second quarter cycle when the fields are decreasing.

Some steps occur also at the smaller radii. The times for the step with a particular submultiple value to occur are often later at these smaller radii. This is consistent with Figs. 11 and 12 where it is seen that for medium and low $B_{z0}$ the smaller radii have greater $\lambda_B$ most of the time. At radii of equal magnitude but different sign, particular submultiples often occur at the same time, but there are periods in the pulse where the times are different. These periods coincide with times when the center of the discharge ($B_\theta=0$) has moved appreciably away from the mean position.

It should be noted that the effect referred to in 3.2, in which it was pointed out that $B_\theta$ stays constant or varies only slightly at the outer radii while $B_\theta$ is increasing rapidly at the inner radii, is synonymous with the steps on the $B_\theta$ waveforms referred here. That is, the constant value, or slow increase, constitutes one or more of the steps on the oscillogram. Thus, in Fig. 10, at the time when $\lambda_B$ is decreasing rapidly at $r=-2.5$ and $-1.5$ cm, the value at $r=3.5$ cm is staying approximately constant near the first harmonic of the Kruskal limit, i.e., 80 cm.

## 4. THEORY

### 4.1. Field Penetration and Enhancement

The penetration of $B_\theta$ into a cylindrical conductor with uniform and constant conductivity has been calculated by Adlam and Tayler.[16] They found that practically complete penetration occurs in about one-fifth of the characteristic time $4\pi\sigma a^2$, where $\sigma$ is the conductivity in emu and $a$ is the radius of the conductor. An estimate of the conductivity in the present experiment can be obtained from the resistance of the gas at peak current. The value is about $2\times10^{-7}$ emu and, assuming the conductivity to be similar during the first few microseconds, the value of $4\pi\sigma a^2/5$ is 6 $\mu$sec. This is not much greater than the observed penetration time of 4 $\mu$sec at high values of $B_{z0}$, but is much greater than the times for low fields. The following theory is put forward to explain the rapid penetration of $B_\theta$ at low $B_{z0}$ and the enhancement of $B_z$.

[16] J. H. Adlam and R. J. Tayler, Atomic Energy Research Establishment Report AERE-T/M 160, 1958 (unpublished).

The electric field applied to a pinch discharge causes the plasma particles to have inward velocities approximately equal to $|\mathbf{E}\times\mathbf{B}|/B_2\equiv E_\perp/B$. It is usually assumed that this inward movement generates a pressure gradient which halts the radial contraction. If there is no appreciable electron temperature gradient and $j_r=0$ there will then be a current perpendicular to both $\mathbf{B}$ and the radius, such that the effective conductivity in this direction, namely $\sigma_\perp(\equiv j_\perp/E_\perp)$ will be approximately $\sigma_{11}/2$, where $\sigma_{11}$ is the conductivity parallel to a magnetic field (see Bickerton[12]). However, this perpendicular current component is generated really by the pressure gradient and not by $E_\perp$.

Here it is postulated that large pressure gradients are prevented either by instabilities or by distortions in the magnetic field. In this case the current density (or the effective conductivity) perpendicular to the magnetic field will remain small. More precisely, since

$$j_\perp=|\nabla p\times\mathbf{B}|/B^2 \quad \text{and} \quad j_{11}=\sigma_{11}E_{11},$$

then the condition

$$|j_\perp|\ll|j_{11}| \tag{1}$$

will be satisfied when

$$|dp/dr|\ll|\sigma_{11}E_{11}B|. \tag{2}$$

It is assumed that one of the above mechanisms keeps the pressure gradient sufficiently low to satisfy condition (2).

An example mechanism leading to such a limitation on the pressure gradient would be an interchange instability. In such an instability there are regions where there is a space charge electric field perpendicular to $\mathbf{B}$ in the reverse direction to the applied $E_\perp$. The outward radial movement of particles in these regions can cancel the inward flux of particles in the intervening regions. Alternatively, distortion of the ideal magnetic field configuration, caused for example by gaps in the coils or by gaps in the metal screen, can in certain circumstances lead to the magnetic lines of force in the discharge being connected to the tube wall.[17] In this case motion of plasma along the lines of force will prevent the generation of a large radial pressure gradient. (These mechanisms are discussed further in Sec. 4.2 below.)

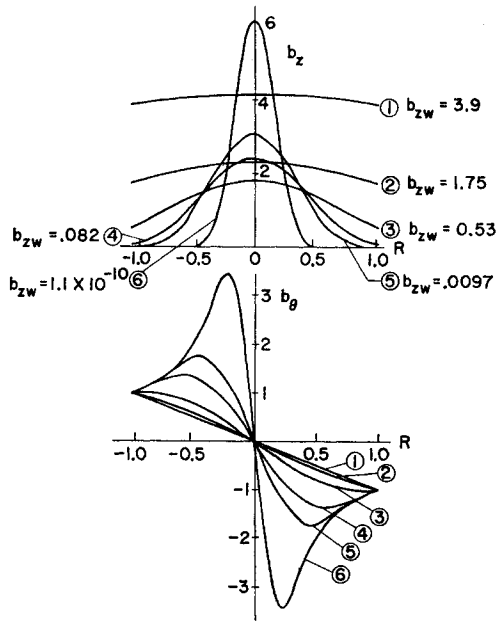


FIG. 14. Example solutions to Eqs. (5) and (6) for the values of $b_{zw}$ indicated. ($b_z=B_z/B_{\theta w}$, $b_\theta=B_\theta/B_{\theta w}$, $R=4\pi\sigma_{11}E_z r/B_{\theta w}$ and $B_{\theta w}$ is the value of $B_\theta$ at tube wall.)

When condition (1) is satisfied, the components of Maxwell's curl $\mathbf{B}$ equation reduce to

$$\frac{1}{r}\frac{\partial(rB_\theta)}{\partial r}=4\pi\sigma_{11}\left\{E_z\frac{B_z^2}{B^2}+E_\theta\frac{B_\theta B_z}{B^2}\right\}, \tag{3}$$

$$-\frac{\partial B_z}{\partial r}=4\pi\sigma_{11}\left\{E_z\frac{B_\theta B_z}{B^2}+E_\theta\frac{B_\theta^2}{B^2}\right\}. \tag{4}$$

### *a. Enhancement of $B_z$ and the Field Profiles at Peak Current*

The solution of Eqs. (3) and (4) for the conditions close to peak current will be considered first. Experimentally the components of $\partial\mathbf{B}/\partial t$ are then observed to be small, so that $E_z$ is approximately constant with respect to radius and $E_\theta\ll E_z$. Hence, if we neglect the $E_\theta$ terms and assume that $\sigma_{11}$ is the same at all radii, Eqs. (3) and (4) reduce to the simple dimensionless forms

$$R^{-1}\partial(Rb_\theta)/\partial R=b_z^2/b^2, \tag{5}$$

$$-\partial b_z/\partial R=b_\theta b_z/b^2, \tag{6}$$

where $b_\theta=B_\theta/B_{\theta w}$, $b_z=B_z/B_{\theta w}$, $b=B/B_{\theta w}$ and $R=4\pi\sigma_{11}E_z r/B_{\theta w}$, where $B_{\theta w}$ is the value of $B_\theta$ at the discharge tube wall.

Equations (5) and (6) have been solved on a computer. Various boundary conditions have been applied at $R=0$, being chosen to give different values of the ratio $b_z/b_\theta$ at $R=1$, which was the radius taken for the tube wall. Some results are shown in Fig. 14.

The large enhancement of $b_z$ within the discharge for low values of $b_{zw}$ is immediately obvious. This enhancement is compared with experiment in Fig. 8, where the theoretical $B_{z0}$ and $B_z$ have been calculated from $b_z$ taking as $B_{\theta w}$ the experimental values computed from peak current measurements (Fig. 8). In other words, the scaling factor $\sigma_{11}E_{11}$ has been chosen to give the same total current in the tube. Qualitatively, the shape of the theoretical curve in Fig. 8 agrees very well with experiment; even the small bump at $B_{z0}=1$ kgauss is reproduced. Quantitatively the predicted fields are higher than the observed fields, the error varying from 13% at 12 kgauss to 40% at 300 gauss.

[17] D. W. Kerst and T. Ohkawa, Bull. Am. Phys. Soc. **6**, 290 (1961).

In Fig. 15 the theoretical profiles for $B_z$ and $B_\theta$ are compared with the experimental points for the case $B_{z0}=170$ gauss, $t=7.6$ $\mu$sec. It can be seen that there is reasonably good agreement in the magnitude of both $B_\theta$ and $B_z$ at all radii. In particular, since the theoretical values of $B_z$ exceed the observed values, the theory is an adequate explanation of the enhancement of $B_z$.

There are several possible reasons why the discharge produces less $B_z$ than predicted by the present theory. For example, $\sigma_{||}$ has been assumed constant with respect to radius. If $\partial T_e/\partial r$ should be a negative, the current density will be larger in the central part of the discharge, and smaller in the outer regions, than that given by the theory. Since $j_z$ is the main component of $\mathbf{j}$ in the center and $j_\theta$ has its maximum in the outer regions, such a negative temperature gradient would result in less $\theta$ currents and hence less $B_z$, for a given total current in the $z$ direction. Secondly, the instabilities may not reduce $|dp/dr|$ accurately to zero. Thus, for example, interchange modes in a discharge with constant magnetic pitch would reduce the pressure gradient only to the marginal stability value $2\gamma pB_\theta^2/r(B^2+\gamma p)$, and pressure gradients of this magnitude have been observed experimentally (see Ware[14]). The presence of a negative pressure gradient would result in less enhancement of $B_z$ for a given gas current.

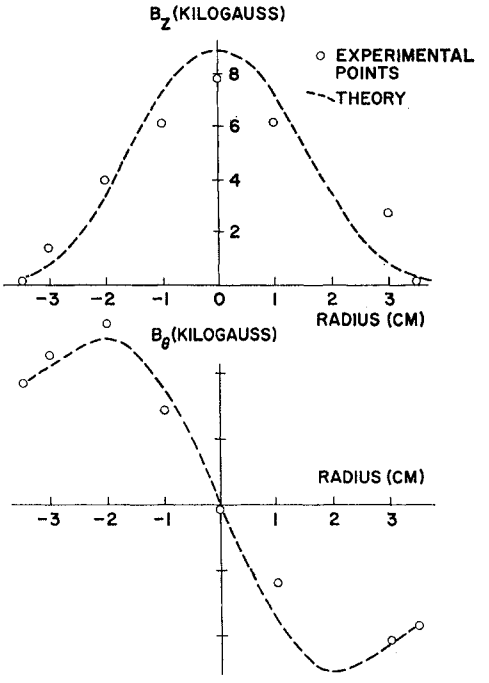


FIG. 15. Comparison between theory and experiment for the radial variation of $B_z$ and $B_\theta$. The experimental points are for $B_{z0}=0.17$ kgauss, $t=7.6$ $\mu$sec.

### *b. Penetration of $B_\theta$*

In order to predict the rate of penetration of $B_\theta$, Eqs. (3) and (4) must be solved simultaneously with Maxwell's equation for curl $\mathbf{E}$. This has not yet been carried out, but the following qualitative discussion shows that a more rapid penetration is predicted for low $B_{z0}$.

Firstly, for $B_z \gg B_\theta$ the term containing $E_\theta$ in Eq. (3) will be small, and the first term will be approximately equal to $4\pi\sigma_{||}E_z$. In this case, therefore, $B_\theta$ will penetrate at the same rate as into a normal conductor with an isotropic conductivity $\sigma_{||}$. At low $B_z$, however, the effective conductivity in the first term in Eq. (3) will be reduced by the factor $B_z^2/B^2 \simeq B_z^2/B_\theta^2$ and hence as far as this term is concerned the penetration will be more rapid. Further, since $B_z$ is increasing in the discharge, $E_\theta$ will have a negative value and will make the second term in Eq. (3) negative. Hence, at any instant of time when the values of $B_\theta$, $B_z$ and $\partial B_\theta/\partial r$ are given, $E_z$ must have a larger value in order to satisfy Eq. (3). That is, the effect of the second term is to make $\partial B_\theta/\partial t$ larger. Both terms, therefore, have the effect of causing a more rapid penetration of $B_\theta$.

## 4.2. Steps on the Magnetic Field Oscillograms

When $\lambda_B=mL/n$, where $m$ and $n$ are integers, the magnetic lines of force are degenerate and join on themselves after $m$ circuits of the torus. As a result, perturbations to the magnetic field at one or more points around the torus will have similar periodicity to the helical lines of force. If $\lambda_B$ is the same at all radii, this resonance between the disturbance and the lines of force can cause all the lines of force within the torus to be connected to the torus wall. The number of circuits of the torus a line of force must make before it reaches the wall will be smaller the larger the magnitude of the disturbing fields. If $\lambda_B$ varies with radius the perturbations have less effect and there may be a region in the discharge where the lines of force have no connection with the walls. (These effects are considered in more detail elsewhere by Kerst and Ohkawa.[17])

Thus at the critical values of $\lambda_B$ there will be a loss of plasma along the lines of force. However, since the perturbing fields at the gaps were very small and the maximum was at the pumping port where they were measured to be no greater than 6%, even in the worst case the lines of force would have to make several circuits of the torus before traversing an appreciable radial distance. The time constant for loss along the lines of force would therefore exceed the torus circumference divided by the ion thermal velocity, which is of the order of 10 $\mu$sec. The steps show appreciable effects occurring in times of the order of 0.5 $\mu$sec and less. It seems unlikely, therefore, that loss along the lines of force is the cause of the steps.

A more likely explanation is a form of instability which has a wavelength related to $\lambda_B$. In the Stellarator experiments of Bernstein *et al.*,[6] steps were observed on the gas current oscillograms at current values such that $\lambda_B$ at the edge of the discharge was a multiple of $L$, i.e.,

$\lambda_B = nL$, where $n = 1, 2, 3$, etc.[18] These steps were correlated with the current ranges during which the magnetohydrodynamic kink instability modes with $m = 1, 2, 3$, etc., were observed respectively. It is attractive, therefore, to look to kink instability for the cause of the present steps.

For currents such that $\lambda_B < L$ the most likely magnetohydrodynamic kink instability is the $m = 1$ mode. For discharges which have a diameter close to that of the surrounding conducting metal sheath, this mode is unstable for only a limited range of the instability wavelength ($2\pi/k$). For example, Tayler[19] has shown that a discharge, which has half of the diameter of the metal tube and which has a uniform current density in the $z$ direction and constant $B_z$ throughout the tube, is unstable for the approximate range $\lambda_B/2 < 2\pi/k < 5\lambda_B$. Within this range the growth rate goes to zero at the singular condition $2\pi/k = \lambda_B$, and the most unstable wavelength is just less than $2\lambda_B$.

If such a discharge is considered in a torus with circumference $L$, then as the current is increased, keeping $B_z$ constant, the discharge will first become unstable to the $m = 1$ kink instability when $\lambda_B = 2L$ and the instability wavelength will be $L$. This wavelength will continue to be the most unstable, until the current has reached the value such that $\lambda_B \simeq L/2.5$ when $L/2$ will become the most unstable wavelength. When $\lambda_B \simeq L/4.5$ the wavelength $L/3$ will become the most unstable, and so on. Changes to a new wavelength would, therefore, be expected at $\lambda_B = 2L$, $L/2.5$, $L/4.5$, etc., and some form of step might be expected on the oscillograms at these values of $\lambda_B$.

These are not the right values to explain the observed steps. However, Tayler's work indicates that as the ratio of the discharge diameter to metal tube diameter is increased the range of unstable wavelengths will become less, and the most unstable wavelength will be closer to $\lambda_B$. The present discharges filled the whole of the tube. Also the fact that $B_z$ is not uniform but decreases with radius may further reduce the instability range. However, the range would have to be markedly reduced, and the most unstable wavelength would have to be very close to $\lambda_B$, to explain the observed steps. Only further theoretical work on the stability of discharges with this configuration can answer this question.

An alternative explanation for the steps can be found in the other type of magnetohydrodynamic instability, the interchange modes.[20] The crests and troughs of such modes have the same helical pitch as the magnetic field. In discharges with magnetic pitch varying only slowly with radius, such modes can be expected to occur over limited annular regions. A further condition for such modes to occur in a toroidal discharge is that the magnetic lines of force should join on themselves or at least approximately do so, that is $\lambda_B \simeq mL/n$, where $m$ is the mode number of the instability and $n$ is the number of instability wavelengths around the circumference $L$.

It is suggested that an interchange instability occurring over a region of discharge would tend to keep the pitch of the lines of force constant in time within this region until conditions were such as to stabilize the mode. The current would then rise fairly rapidly until $\lambda_B$ was reduced to the next harmonic value so that an interchange instability with one more wavelength in the $z$ direction could occur. Thus steps would be produced at $\lambda_B = mL/n$, and in particular the experimental results would be explained by modes with $m = 1$ and 2. Further, an interchange mode with a given wavelength would occur at a later time at small radii since the values of $\lambda_B$ are larger there and reach the critical value later. Corresponding steps would therefore occur later, as observed experimentally.

### 4.3. Disturbing Effect of the Magnetic Probe Tube

All the experimental observations reported in this paper were made with the magnetic probe present in the discharge, and hence the results apply to such a disturbed discharge. One effect of the probe tube is to cast a "shadow" in the plasma, i.e., a region of lower particle density. This shadow, which was first observed by Tonks,[21] runs parallel to **B** in the opposite direction to $j_{11}$. Since the probe tube extends across the whole width of the discharge the shadow will cause an $m = 2$ perturbation to the plasma density and pressure in the vicinity of the probe. Secondly the tube surface will get hot, outgas and possibly vaporize, causing impurities to enter the discharge. Measurements made with a thermocouple inserted into the probe tube showed a 10°C rise in temperature for a single discharge. Assuming that the heat given to the probe tube is deposited uniformly over the tube surface and at a constant rate throughout the current pulse, a thermal conduction calculation shows that $T_s$, the temperature of the tube surface exposed to the discharge, would be 600°C at peak current. ($T_s$ is proportional to $t^{\frac{1}{2}}$ while the pulse is being applied.) Such a temperature will not vaporize the alumina, but considerable outgassing can be expected. After a number of discharges the gas involved will probably be mainly hydrogen.

Here the important question is whether the probe appreciably affects the magnetic field configuration or in any way causes the observed effects such as the low pressure gradient or the waveform steps. Unfortunately insufficient measurements were made to answer this question for the present discharge. In general, however,

[18] This condition has been modified here to the case for no externally applied rotational transform. The observed values for the start of a step were given by $\lambda_B(ni/2\pi + h) = nL$, where $i$ is the rotational transform angle, and $n$ and $h$ are integers.

[19] R. J. Tayler, Proc. Phys. Soc. **B70**, 1049 (1957).

[20] J. L. Johnson, C. R. Oberman, R. M. Kulsrud, and E. A. Frieman, reference 1, Vol. 31, p. 198.

[21] L. Tonks, Phys. Rev. **59**, 522 (1941).

other workers using magnetic probes in toroidal discharges[22–24] have found that the main properties of the discharge, including current amplitude, resistance, and ion temperature are not greatly affected by a probe, at least during the first part of the pulse up to peak current and provided excessive powers are not used. (The nuclear reaction rate in the vicinity of the probe is the one property greatly affected by the presence of a probe.[10]) With Zeta[24] the field measurements of one probe were not altered in general shape by the insertion of a second probe further along the tube. That waveform steps occur in the absence of a probe is seen from the work of Butt,[11] who observed them on the current waveforms. Also the instability modes reported by Bernstein *et al.*[6] appeared both with and without a probe in the discharge.

It can be inferred from these results that, in most cases, although probes do affect the discharge to some extent, they do not alter its general character. However, because of the differences in discharge tube size and design, these results with other experiments do not prove that the present discharge was not an exception.

## 5. CONCLUSIONS

For values of the applied magnetic field ($B_{z0}$) comparable with or less than the peak value of $B_\theta$ at the tube wall, the $B_\theta$ fields penetrate into the discharge faster than expected from simple electromagnetic theory. In addition, there is a generation of $B_z$ flux within the discharge. Both the rate of penetration of $B_\theta$ and the generation of $B_z$ are greater the lower the value of $B_{z0}$. Steps are observed on the magnetic field oscillograms when the magnetic pitch satisfies $\lambda_B = L/n$ or $L/2n$. These results apply to a discharge with a magnetic probe tube passing through it.

If instabilities are assumed to prevent appreciable pressure gradients being generated in the discharge, then the current density perpendicular to **B** will be small. In this case the currents produced parallel to **B** by the applied electric field $E_z$ (assumed constant with respect to radius) give magnetic field configurations in good agreement with those observed experimentally after the $B_\theta$ penetration is complete. In particular the spectacular production of $B_z$ flux for low values of $B_{z0}$ is satisfactorily explained. Further, the assumption that $j_\perp$ is small leads to a qualitative explanation of the rapid penetration of $B_\theta$.

A further conclusion from this theory is that neither the sudden production of $B_z$ flux in a discharge nor its continuous enhancement in slow discharges is necessarily evidence for an $m=1$ kink instability. Any instability, or field distortion, which keeps $\nabla p$ small will produce these effects.

The most likely instability which is keeping $\nabla p$ small in the experiments reported here, and which would explain the oscillogram steps, is the magnetohydrodynamic interchange modes with $m=1$ and $m=2$.

## ACKNOWLEDGMENTS

The authors gratefully acknowledge the assistance of John Malmberg and Ed Dacus, who were responsible, respectively, for the design and construction of the multicoil magnetic probe.

The authors also wish to thank for his help and encouragement, Don Kerst, under whose direction this research was carried out.

[22] N. L. Allen and B. S. Liley, reference 11, Vol. 2, p. 937.
[23] T. P. Hughes, Associated Electrical Industries Report AEI-A.1145, 1961 (unpublished).
[24] G. N. Harding, A. N. Dellis, A. Gibson, B. Jones, D. J. Lees, R. W. P. McWhirter, S. A. Ramsden, and S. Ward, reference 1, Vol. 32, p. 365.

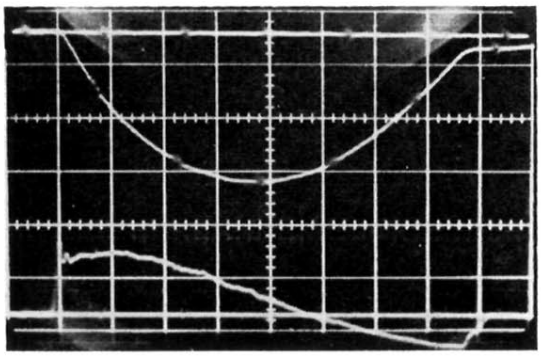

FIG. 1. Example oscillograms for the total gas current in the $z$ direction ($J_z$) and the voltage applied to the torus. The upper trace is $J_z$. The time base is 2 $\mu$sec per major division.

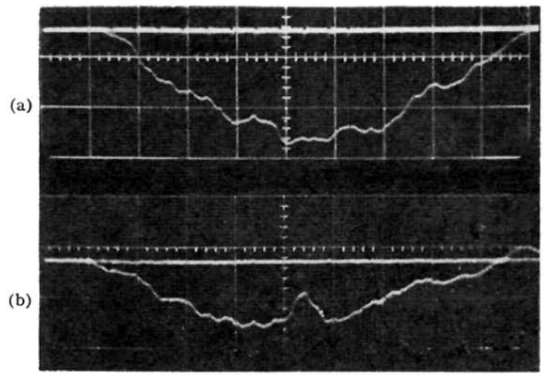


FIG. 13. Two examples of clearly defined steps on the $B_\theta$ waveform. Both are at the radius $-3$ cm. (a) $B_{z0}=8$ kgauss, (b) $B_{z0}=13$ kgauss.

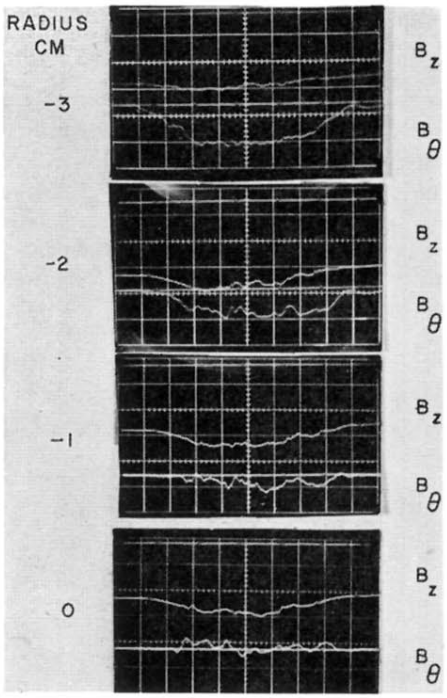


FIG. 2. Oscillograms for $B_z$ and $B_\theta$ at the radii indicated when the applied field ($B_{z0}$) was 11.6 kgauss.

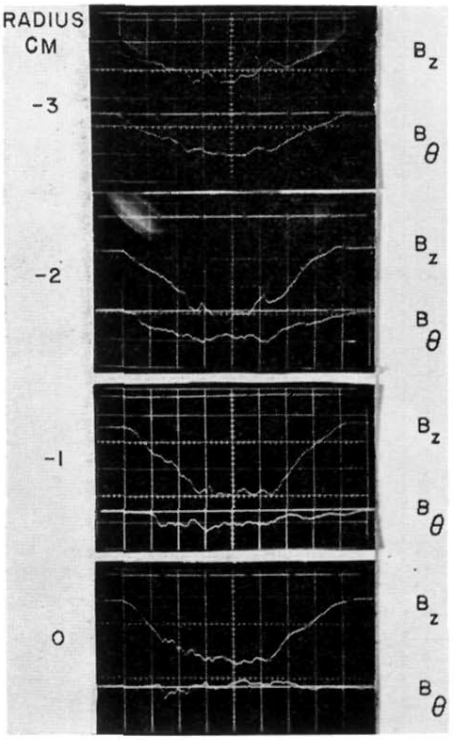


FIG. 3. Oscillograms for $B_z$ and $B_\theta$ when $B_{z0}$ was 2.6 kgauss.

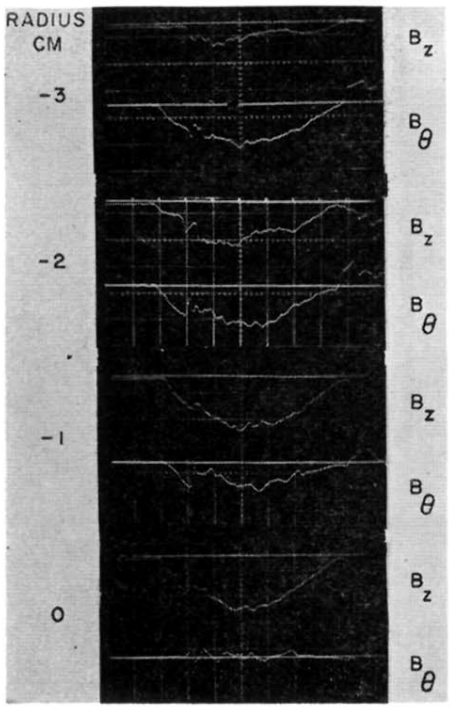


FIG. 4. Oscillograms for $B_z$ and $B_\theta$ when $B_{z0}$ was 0.3 kgauss.